

REAL-TIME CONTROLLER-HARDWARE-IN-THE-LOOP TESTING OF DC MOTOR-DRIVE SYSTEMS

Fazel Mohammadi¹ , Rasoul Bok²

¹ Electrical and Computer Engineering and Computer Science Department, University of New Haven, West Haven, CT 06516, USA

² Department of Electrical and Computer Engineering, Isfahan University of Technology, Isfahan 84156-83111, Iran

f Mohammadi@newhaven.edu, fazel.mohammadi@ieee.org, rasool.bok@ec.iut.ac.ir

DOI: 10.15598/aece.v22i1.5720

Article history: Received Jan. 26, 2024; Revised Feb. 19, 2024; Accepted Mar. 23, 2024; Published Mar. 31, 2024.

This is an open access article under the BY-CC license.

Abstract. This paper aims at validating and performance testing of the real-time models for Direct Current (DC) motor-drive systems using Controller-Hardware-in-the-Loop (C-HIL) platform. The DC motor-drive systems are modeled in real-time using STM32F4 Discovery kits, where a minimum time-step of 10 μ s is achieved. The closed-loop control scheme is based on adjusting the angular velocity of the DC motor by controlling the armature current, which in turn, controls the developed electromechanical torque of the DC motor. Implementation and performance verification of DC motor-drive systems and the controller can be time-consuming and expensive. The main objective of this paper is to demonstrate the practicality of real-time implementation and performance verification of DC motor-drive systems using the C-HIL testing platform to show perfect concordance with the machine theory without the need for costly commercial real-time simulators.

Keywords

Controller-Hardware-in-the-Loop (C-HIL), Digital Control, Power Drive Systems, DC Motors.

1. Introduction

Over the past decade, there has been a growing demand for more high-efficient high-performance electric motor-drive systems, which require more complex

power electronics control systems [1–4]. The adoption of wide-bandgap semiconductor materials, such as Gallium Nitride (GaN) and Silicon Carbide (SiC), allows for high switching frequencies, resulting in more complicated challenges for developing electric motor-drive systems [5, 6]. To address such challenges, Hardware-in-the-Loop (HIL) testing can be utilized to assess the performance of the process-actuator system, also known as a plant, and the supervisory control algorithms [7]. HIL technology enables more efficient and economical implementation of electric drive-motor systems by building digital prototypes instead of real experimental setups. Considering high-voltage high-power electric drive-motor systems, building the system's prototypes is a time-consuming and expensive process. In this regard, HIL technology facilitates performing exhaustive testing with a high degree of safety at a reduced cost.

Commercial real-time simulators, such as OPAL-RT Simulator, provide accurate and safe development and testing of complex control, protection, and monitoring systems [8] [9]. However, performing HIL testing with commercial real-time simulators is an expensive and time-consuming process. An alternative method is Controller-Hardware-in-the-Loop (C-HIL) testing, which is an effective and safe solution for high-fidelity testing of controllers at a fraction of the cost. Figure 1 illustrates how digital hardware can be utilized to emulate various system components, including but not limited to controllers, power electronic devices, etc., in a safe environment. As shown in this figure, the C-HIL testing platform consists of two layers, referred to as cyber and physical layers. The physical layer includes

accurate models of all system components, including power electronic devices, DC motors, etc., which are stable, predictable, and reliable. The cyber layer cannot have an accurate model as it is constantly evolving, unpredictable, vulnerable to cyberattacks, vulnerable to incorrectly being programmed by technicians, and it may have many versions of software, firmware, and even controller types. Thus, the actual controller cannot be simulated. In this regard, the actual controller is linked to a digital emulation of an actual system, i.e., HIL, in closed-loop to create a digital twin that allows for high-fidelity testing. It should be noted that the HIL model in Figure 1 is mainly a set of differential equations representing the mathematical model of the actual system and solved in a short time-step. A typical Central Processing Unit (CPU)-based real-time simulation can achieve a minimum time-step of $\geq 10 \mu s$ due to the large bus latency in a CPU [10]. To accurately model the behavior of a system, the simulation frequency should be substantially higher than the input frequency of the system. In general, in order to perform C-HIL testing of power converters, a time-step of $\ll 10 \mu s$ is required. Additionally, the exchanged signals between the control system and the HIL model are of low power and voltage, creating an environment, which is both secure and non-destructive, to design, implement, and assess the performance of control systems [11]– [13].

A promising approach to solve the problems related to consistently-high latency in CPU-based HIL testing is to use Field-Programmable Gate Arrays (FPGAs) [14]. Such devices provide multiple advantages, including low latency, parallel processing capability, and high performance and energy efficiency, while their main drawbacks are low-level programming and relatively high cost. In [15], an FPGA-based real-time platform for the simulation of power converters and electric machines is presented. As stated in [15], it is possible to achieve the time-step of 200 ns to model power converters and electric machines. In addition, the real-time simulation of Alternating Current (AC) machine transients in an FPGA-based real-time simulator is presented in [16], where a computation time of 44 ns within the simulation time-step is achieved. Rather than FPGAs, it is possible to achieve a time-step of 1 μs using programmable Digital Signal Processors (DSPs) for real-time simulation of power converters. However, DSPs are slower than FPGAs, they can be programmed easily at a lower cost of implementation.

Based on the above analysis, this paper aims at validating and performance testing of real-time implementation of DC motor-drive systems using the proposed C-HIL testing platform. In this regard, the real-time models for DC motor-drive systems (HIL model) and the control scheme are implemented in two STM32F4

Discovery kits. The HIL model and the controller are interconnected via Analog-to-Digital Converter (ADC) and Digital-to-Analog Converter (DAC) pins. In particular, the angular velocity and armature current are the two signals, which are sent to the controller using DAC pins, and the controller generates the control signals, i.e., the duty cycle of Insulated-Gate Bipolar Transistor (IGBT) switching devices, using ADC pins. The simulation and experimental results verify the applicability and effectiveness of the proposed C-HIL testing platform to be used for validating the performance of new control strategies for electric drive systems.

In summary, the main contributions of this paper are as follows:

- Implementation of real-time models for DC motor-drive systems using STM32F4 Discovery kits
- Validating and performance testing of the real-time models for Direct Current (DC) motor-drive systems using a closed-loop angular velocity controller
- Comparing the simulation results with experimental results to verify the performance of the proposed C-HIL testing platform

The rest of this paper is organized as follows. Modeling and control of DC motor-drive systems are presented in Section 2. Simulation and experimental results are provided in Section 3. Finally, Section 4. Concludes this paper.

2. Modeling and Control of DC Motor-Drive Systems

2.1. Modeling of a DC Motor

The separately-excited DC motor has two distinct voltage sources supplying power to its field and armature circuits. Figure 2 illustrates a typical structure of a DC motor-drive system for dynamic analysis. In this figure, I_a , R_a , and L_a are the current, resistance, and inductance of the armature, respectively. In addition, V_f , R_f , and L_f indicate the voltage, resistance, and inductance of the field circuit, respectively. Finally, E_a , V_t , V_{DC} , and ω_m are the internal voltage of the DC motor, the voltage at the DC motor terminals, DC voltage source feeding the DC motor, and the angular velocity of the DC motor shaft, respectively.

Applying Kirchhoff's voltage law to the armature circuit leads to deriving the following expression [17].

$$V_t = R_a i_a(t) + L_a \frac{di_a(t)}{dt} + E_a(t) \quad (1)$$

where $E_a(t)$ is the back Electromotive Force (EMF), which is proportional to the angular velocity of the DC

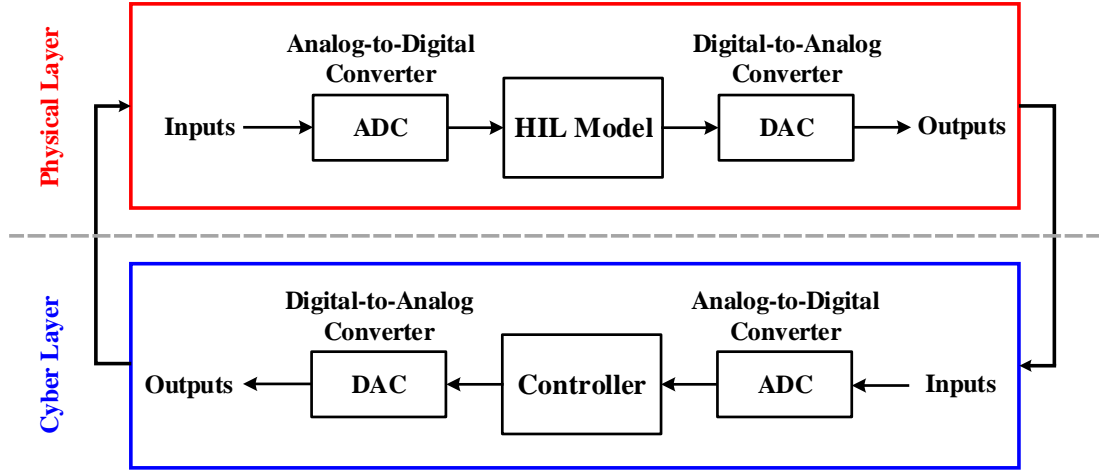


Fig. 1: The generalized C-HIL setup.

motor shaft and the field current, and can be expressed as follows:

$$E_a(t) = L_{af} I_f(t) \omega_m(t) \quad (2)$$

where L_{af} is the field-armature mutual inductance.

For motoring operation, the developed electromechanical torque by the DC motor highly depends on the armature current and field current, and it can be expressed as follows:

$$T_e(t) = L_{af} I_f(t) I_a(t) \quad (3)$$

By adjusting the voltage at the DC motor terminals (V_t), the DC motor angular velocity gradually varies from zero to its predetermined angular velocity at the constant torque region. An increase in V_t leads to an increase in the armature current, which in turn, increases the developed electromechanical torque and the DC motor angular velocity. Thus, the following expression can be written to demonstrate the relationship between the DC motor angular velocity, the developed electromechanical torque, and the load torque (T_L).

$$J \frac{d\omega_m(t)}{dt} = T_e(t) - T_L(t) - B_m \omega_m(t) \quad (4)$$

where J is the moment of inertia of the DC motor and B_m is the viscous friction coefficient.

According to Equations (1)–(4), the discrete model of the DC motor can be represented by the following expressions.

$$V_t(k) = V_{DC} D(k) \quad (5)$$

$$\frac{dI_a(k)}{dk} = \frac{1}{L_a} (V_t(k) - E_a(k-1) - R_a I_a(k-1)) \quad (6)$$

$$\frac{dI_f(k)}{dk} = \frac{1}{L_f} (V_f - R_f I_f(k-1)) \quad (7)$$

$$J \frac{d\omega_m(k)}{dk} = T_e(k-1) - T_L(k) - B_m \omega_m(k-1) \quad (8)$$

Integrating Equation (6)–(8) using the rectangular integration method (Backward Differencing), the model can be solved based on the following expressions.

$$\begin{cases} I_a(k) = I_a(k-1) + \frac{dI_a(k)}{dk} \\ I_f(k) = I_f(k-1) + \frac{dI_f(k)}{dk} \\ \omega_m(k) = \omega_m(k-1) + \frac{d\omega_m(k)}{dk} \\ E_a(k) = L_{af} I_f(k) \omega_m(k) \\ T_e(k) = L_{af} I_f(k) I_a(k) \end{cases} \quad (9)$$

2.2. Control of DC Motor-Drive Systems

As shown in Figure 3, the proposed control system comprises two primary control loops. The external control loop is utilized to control the angular velocity of the DC motor and to minimize the error between the measured angular velocity of the DC motor and its reference value. As previously stated, the armature current can be adjusted to control the developed electromechanical torque, which in turn, allows for controlling the angular velocity of the DC motor. In this regard, the output of this control loop determines the reference value of the armature current. The internal control loop adjusts the armature current by minimizing the error between the measured armature current of the DC motor and the reference value generated by the external loop using a Proportional-Integral (PI) controller. The output of this control loop is the duty cycle of the power converter, as shown in Figure 3.

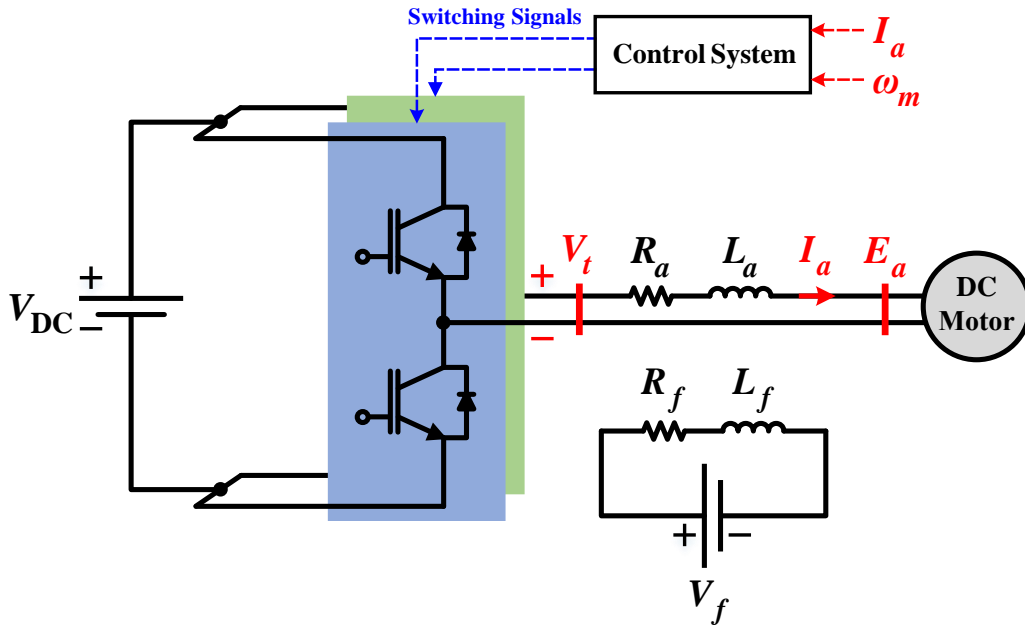


Fig. 2: The typical structure of a DC motor-drive system for dynamic analysis.

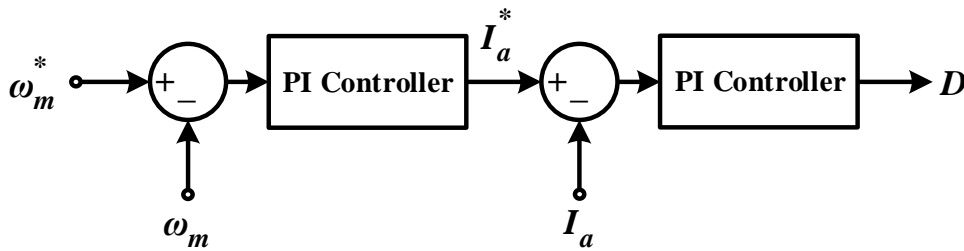


Fig. 3: The block diagram of the control scheme for DC motor-drive systems.

3. Results and Discussion

3.1. Simulation Results

In order to assess the performance of the proposed C-HIL testing platform, the DC motor-drive systems shown in Figure 2 are initially simulated in MATLAB/Simulink environment. The parameters of the DC motor are shown in Table 1.

The simulation results for DC motor-drive systems in different scenarios with a sample time of $10 \mu s$ are shown in Figure 4. The control system is designed to ensure that the angular velocity of the DC motor maintains a predefined value (reference value). Therefore, by adjusting the voltage at the DC motor terminals and the armature current, the angular velocity of the DC motor can be controlled. It should be noted that the gains of the speed controller and current controller are set to $P = 1.5$ and $I = 1$ and $P = 1$ and $I = 2$, respectively.

Tab. 1: The parameters of the DC motor.

Parameters	Values
Armature Resistance (R_a)	2.581 [Ω]
Armature Inductance (L_a)	2.810 [mH]
Field Circuit Resistance (R_f)	281.375 [Ω]
Field Circuit Inductance (L_f)	156 [H]
Field Circuit Voltage (V_f)	100 [V]
Field-Armature Mutual Inductance (L_{af})	0.572 [H]
DC Voltage Source (V_{DC})	200 [V]
Viscous Friction Coefficient (B_m)	0.00295 [N.m.s/rad]
Moment of Inertia (J)	0.0221 [kg.m ²]

Figure 4(a) illustrates the angular velocity of the DC motor as well as its reference value. According to Figure 4(a), in the first scenario, the reference value of the angular velocity is initially set to $\omega_m^* = 800$ rpm, and the angular velocity of the DC motor follows the reference value. As shown in Figure 4(b), the mechanical load is $T_L = 1$ N.m and remains constant. In the second scenario, starting at $t = 3$ s, the angular velocity

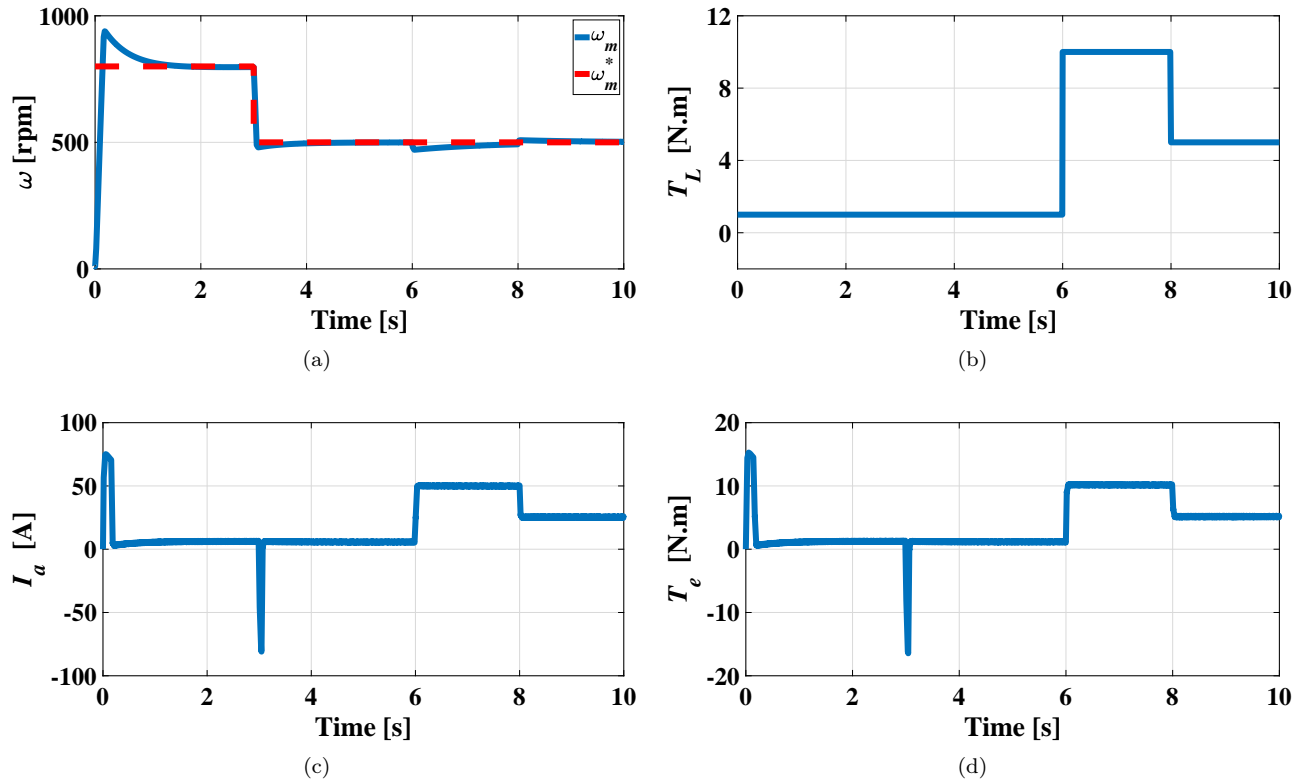


Fig. 4: Simulation results for the angular velocity control of the DC motor: (a) angular velocity (ω), (b) mechanical load (T_L), (c) armature current (I_a), and (d) developed electromechanical torque (T_e).

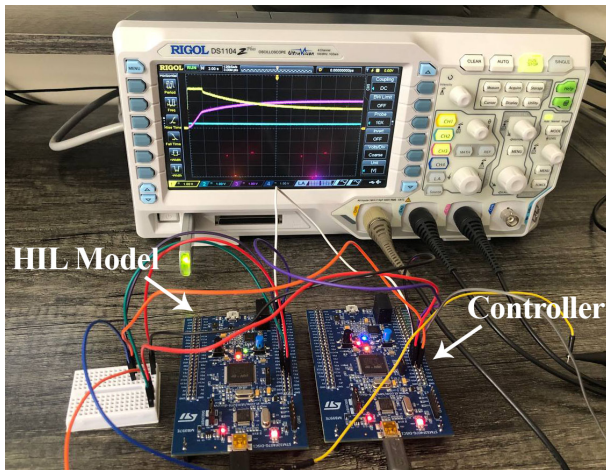


Fig. 5: The experimental C-HIL testbed.

reference value is decreased by 300 rpm and set to 500 rpm. Accordingly, as shown in Figure 4(c) a sudden decrease in the armature current occurs at $t = 3$ s to decrease the developed electromechanical torque and the angular velocity of the DC motor. In the third scenario, at $t = 6$ s, the mechanical load is increased from 1 N.m to 10 N.m with no changes in the reference value of the angular velocity. In order to maintain the angular velocity constant, the controller should increase the developed electromechanical torque to match the me-

chanical load. In this regard, Figure 4(d) shows that the developed electromechanical torque reaches 10 N.m at $t = 6$ s. Consequently, according to Figure 4(c), the controller adjusts the current from 6 A to 50 A by changing the duty cycle of the power converter. In the fourth scenario, as shown in Figure 4(b), the mechanical load is decreased by 5 N.m at $t = 8$ s. Accordingly, the controller decreases the armature current to 25 A to maintain the angular velocity constant.

3.2. Experimental Results

The proposed C-HIL testing platform is illustrated in Figure 5. As shown in this figure, the executable codes from the HIL model of the DC motor-drive systems and the control scheme are deployed to two separate target devices (STM32F4 Discovery kits). As mentioned earlier, the HIL model and the controller operate as a closed-loop system. The closed-loop is implemented when the feedback of the DC motor's angular velocity and armature current is sent to the controller via Digital-to-Analog Converter (DAC) pins, and the control signal, i.e., the duty cycle, is generated by the controller and sent to the HIL model via an Analog-to-Digital Converter (ADC) pin. In order to verify the performance of the proposed C-HIL testing platform,

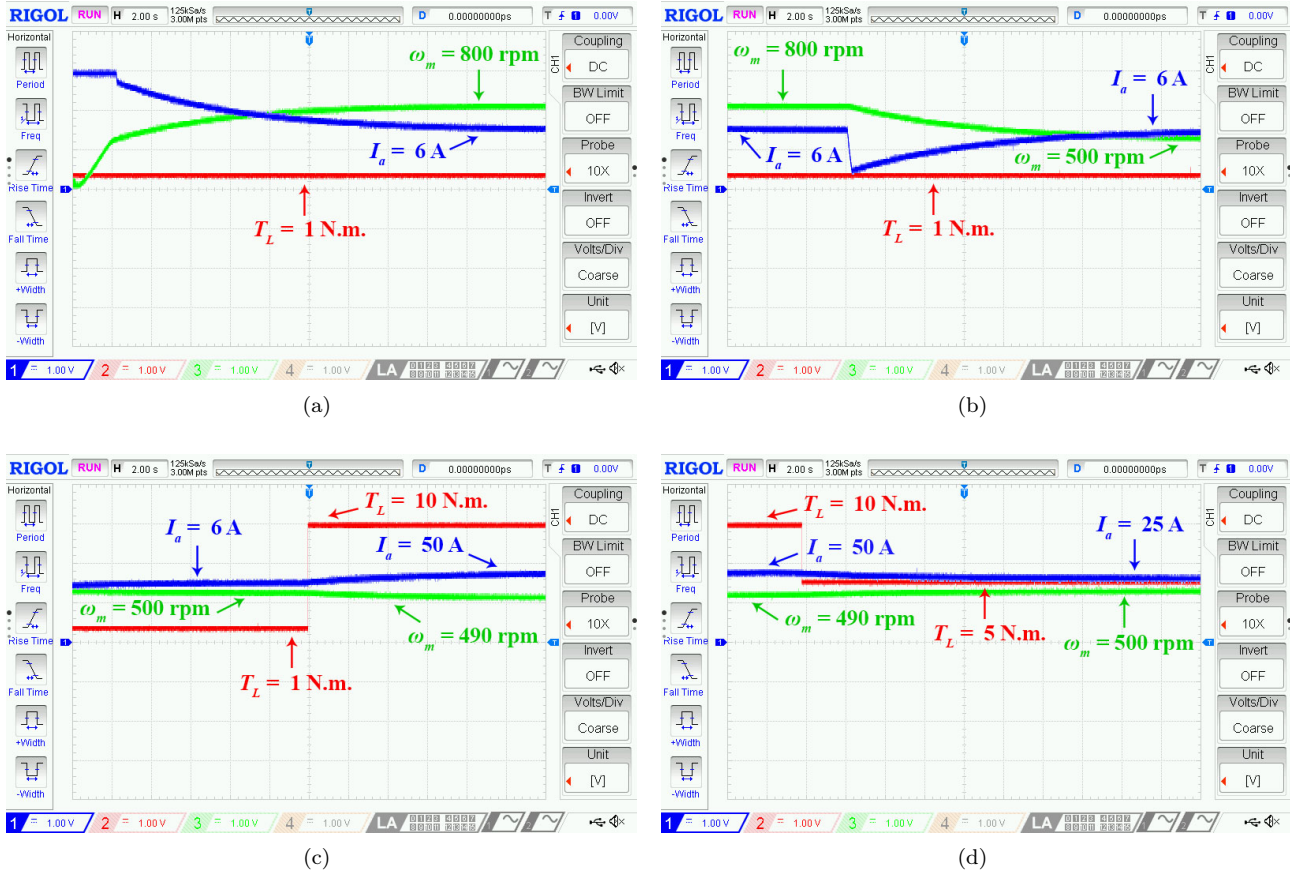


Fig. 6: Experimental results for the angular velocity control of the DC motor.

the same scenarios and same parameters for the DC motor are considered.

Figure 6 shows the experimental results for the DC motor-drive systems with a sample time of $50 \mu s$. Due to the small discrepancy in sample time, the gains of the PI controllers in the simulation and experimental sections slightly differ from each other. In this regard, the gains of the speed controller and current controller are set to $P = 0.2$ and $I = 0.5$ and $P = 0.05$ and $I = 0.5$, respectively. According to Figure 6(a), the reference value of the angular velocity is initially set to $\omega_m^* = 800$ rpm and the mechanical load torque is $T_L = 1$ N.m. Once the angular velocity reaches its reference value, the armature current gradually reaches $I_a = 6$ A. As shown in Figure 6(b), the reference value of the angular velocity is changed in step from 800 rpm to 500 rpm. The controller decreases the armature current of the DC motor to match the angular velocity of the DC motor to its reference value. Since the mechanical load torque is not yet changed, after a few seconds, the armature current reaches 6 A. Figure 6(c) illustrates that once the angular velocity reaches its reference value, a step change from 1 N.m to 10 N.m in the mechanical load of the DC motor is made. According to the obtained results, despite the large increase in the mechan-

ical load of the DC motor, the controller successfully adjusts the angular velocity to its approximately predetermined value by increasing the armature current from 6 A to 50 A. Finally, the mechanical load of the DC motor is decreased by 5 N.m., as shown in Figure 6(d). The controller changes the duty cycle of the power converter to control the developed electromechanical torque by the DC motor, and accordingly, its angular velocity. In this regard, the armature current is decreased from 50 A to 25 A to ensure that the angular velocity of the DC motor maintains a predefined value, i.e., 500 rpm.

3.3. Discussion

While C-HIL testing platforms offer significant advantages in testing and validating control algorithms in a realistic hardware environment, the complexity of hardware integration and synchronization can pose challenges, requiring meticulous attention to real-time communication and data exchange between the controller and physical components. Besides, achieving high-fidelity representation of complex systems in real-time simulations may demand substantial computational resources. Apart from that, the scalability of

C-HIL setups for large-scale systems remains an open issue, particularly in distributed energy systems or interconnected networks [18].

Future work in this domain should focus on developing more efficient and scalable algorithms for real-time simulations, exploring advanced synchronization techniques, and addressing the challenges associated with the integration of emerging technologies, such as Artificial Intelligence (AI) and machine learning, into C-HIL frameworks. Optimization algorithms, such as Multi-Objective Genetic Algorithm (MOGA) [19] and Modified Adaptive Selection Cuckoo Search Algorithm (MASCOSA) [20], can be employed to fine-tune controller parameters and determine the optimal configuration for various components. Enhancements in modeling accuracy, adaptability to dynamic system conditions, and the incorporation of cybersecurity measures are also areas that warrant further research to advance the effectiveness and applicability of C-HIL systems.

4. Conclusions

In this paper, modeling, validation, and performance testing of the real-time models for Direct Current (DC) motor-drive systems using a Controller-Hardware-in-the-Loop (C-HIL) testing platform is provided. The proposed C-HIL testing platform utilizes two STM32F4 Discovery kits for deploying the executable codes related to the real-time models of the DC motor-drive systems and the control scheme. The proposed C-HIL testing platform is capable of adjusting the angular velocity of the DC motor by controlling the armature current, and accordingly, controlling the developed electromechanical torque of the DC motor. The simulation and experimental results verify the performance and applicability of the proposed C-HIL testing platform using two STM32F4 Discovery kits without the need for costly commercial real-time simulators.

Author Contributions

F.M. and R.B. developed the theoretical formalism, performed the analytic calculations, and performed the dynamic simulations and experimental results. Both F.M. and R.B. contributed to the final version of the manuscript. In addition, F.M. supervised the project.

References

[1] Mohammadi, F., Nazri, G.-A., and Saif, M. A Real-Time Cloud-Based Intelligent Car Parking

System for Smart Cities. *2019 IEEE 2nd International Conference on Information Communication and Signal Processing (ICICSP)*, Sep. 2019, DOI: 10.1109/ICICSP48821.2019.8958543.

- [2] Mohammadi, F. and Saif, M. A Comprehensive Overview of Electric Vehicle Batteries Market. *e-Prime - Advances in Electrical Engineering, Electronics and Energy*, Vol. 3, Mar. 2023, DOI: 10.1016/j.prime.2023.100127.
- [3] Mohammadi F., and Saif, M. A Multi-Stage Hybrid Open-Circuit Fault Diagnosis Approach for Three-Phase VSI-Fed PMSM Drive Systems. *IEEE Access*, Vol. 11, Dec. 2023, DOI: 10.1109/ACCESS.2023.3339549.
- [4] Tran, C. D., Kuchar, M., Sobek, M., Sotola, V., and Dinh, B. H. Sensor Fault Diagnosis Method Based on Rotor Slip Applied to Induction Motor Drive. *Sensors*, Vol. 22(22), Nov. 2022, DOI: 10.3390/s22228636.
- [5] Shawlin, S. S., Mohammadi, F., and Rezaei-Zare, A. GPU-Based DC Power Flow Analysis Using KLU Solver. *2022 IEEE International Conference on Environment and Electrical Engineering and 2022 IEEE Industrial and Commercial Power Systems Europe*, Jun.-Jul. 2022, DOI: 10.1109/EEEIC/ICPSEurope54979.2022.9854563.
- [6] Shawlin, S. S., Mohammadi, F., and Rezaei-Zare, A. GPU-Accelerated Sparse LU Factorization for Concurrent Analysis of Large-Scale Power Systems. *2022 IEEE International Conference on Environment and Electrical Engineering and 2022 IEEE Industrial and Commercial Power Systems Europe*, Jun.-Jul. 2022, DOI: 10.1109/EEEIC/ICPSEurope54979.2022.9854600.
- [7] Mohammadi, F., Mohammadi-Ivatloo, B., Gharehpetian, G. B., Hasan Ali, M., Wei, W., Erdinç, O., and Shirkhani, M. Robust Control Strategies for Microgrids: A Review. *IEEE Systems Journal*, Vol. 16(2), Jun. 2022, DOI: 10.1109/JSYST.2021.3077213.
- [8] Mohammadi, F., Nazri, G.-A., and Saif, M. Modeling, Simulation, and Analysis of Hybrid Electric Vehicle Using MATLAB/Simulink. *2019 International Conference on Power Generation Systems and Renewable Energy Technologies (PGSRET)*, Aug. 2019, DOI: 10.1109/PGSRET.2019.8882686.
- [9] Mehdipour, C., Mohammadi, F., and Mehdipour, I. Analytical Approach to Nonlinear Behavior Study of an Electric Vehicle. *2019 6th International Conference on Control, Instrumentation and Automation (ICCIA)*, Oct. 2019, DOI: 10.1109/ICCIA49288.2019.9030985.

- [10] Jalili-Marandi, V., Zhou, Z., and Dinavahi, V. Large-Scale Transient Stability Simulation of Electrical Power Systems on Parallel GPUs. *IEEE Transactions on Parallel and Distributed Systems*, Vol. 23(7), Jul. 2012, DOI: 10.1109/TPDS.2011.291.
- [11] Mohammadi, F., Bok R., and Hajian, M. Real-Time Controller-Hardware-in-the-Loop Testing of Power Electronics Converters. *2022 13th Power Electronics, Drive Systems, and Technologies Conference (PEDSTC)*, Feb. 2022, DOI: 0.1109/PEDSTC53976.2022.9767506.
- [12] Mohammadi, F., Bok, R., Hajian, M., and RezaeiZare, A. Controller-Hardware-in-the-Loop Testing of A Single-Phase Single-Stage Transformerless Grid-Connected Photovoltaic Inverter. *2022 IEEE Texas Power and Energy Conference (TPEC)*, Feb.-Mar. 2022, DOI: 10.1109/TPEC54980.2022.9750851.
- [13] Bok, R., Mohammadi, F., and Hajian, M. A New Multi-Port Interline DC Power Flow Controller for Multi-Terminal HVDC Grids. *e-Prime - Advances in Electrical Engineering, Electronics and Energy*, Vol. 6, Dec. 2023, DOI: 10.1016/j.prime.2023.100363.
- [14] Mojlish, S., Erdogan, N., Levine, D., and Davoudi, A. Review of Hardware Platforms for Real-Time Simulation of Electric Machines. *IEEE Transactions on Transportation Electrification*, Vol. 3(1), Mar. 2017, DOI: 10.1109/TTE.2017.2656141.
- [15] Herrera, L. and Wang, J. FPGA Based Detailed Real-Time Simulation of Power Converters and Electric Machines for EV HIL Applications. *2013 IEEE Energy Conversion Congress and Exposition*, Sep. 2013, DOI: 10.1109/ECCE.2013.6646920.
- [16] Matar, M. and Iravani, R. Massively Parallel Implementation of AC Machine Models for FPGA-Based Real-Time Simulation of Electromagnetic Transients. *IEEE Transactions on Power Delivery*, Vol. 26(2), Apr. 2011, DOI: 10.1109/TPWRD.2010.2086499.
- [17] Sami, S. S., Obaid, Z. A., Muhssin, M. T., and Hussain, A. N. Detailed Modelling and Simulation of Different DC Motor Types for Research and Educational Purposes. *International Journal of Power Electronics and Drive Systems*, Vol. 12(2), Jun. 2021, DOI: 10.11591/IJPEDS.V12.I2.PP703-714.
- [18] Nguyen, T. T. and Mohammadi, F. Cyber-Physical Power and Energy Systems with Wireless Sensor Networks: A Systematic Review. *Journal of Electrical Engineering & Technology*, Vol. 8, Apr. 2023, DOI: 10.1007/s42835-023-01482-3.
- [19] Nguyen, T. T. and Mohammadi, F. Optimal Placement of TCSC for Congestion Management and Power Loss Reduction Using Multi-Objective Genetic Algorithm. *Sustainability*, Vol. 12(7), Apr. 2020, DOI: 10.3390/su12072813.
- [20] Nguyen, T. T., Pham, L. H., Mohammadi, F., and Kien, L. C. Optimal Scheduling of Large-Scale Wind-HydroThermal Systems with Fixed-Head Short-Term Model. *Applied Sciences*, 10(8), Apr. 2020, DOI: 10.3390/app10082964.